

Normal-stress differences and the detection of disclinations in nematic elastomers

ELIOT FRIED & RUSSELL E. TODRES

Department of Theoretical and Applied Mechanics
University of Illinois at Urbana-Champaign
Urbana, IL 61801-2935, USA

We use a continuum model to investigate the isochoric radial expansion of a right circular cylindrical specimen composed of a nematic elastomer that is cross-linked in a uniaxial state and then annealed. Numerical solutions show that, above a certain radial expansion, the material has a definitive energetic preference for a state involving a disclination of strength $+1$ along the cylinder axis. Surrounding such a disclination is a core with radial dimension on the order of 10^{-2} μm , which coincides with observations in conventional liquid-crystal melts. Examination of the normal-stress differences shows that the first of these differences depends non-monotonically on the extent of radial expansion and possesses a local minimum at the point where a disclination becomes energetically preferred. This suggests a practical experimental method for testing the predictions of our model.

Keywords: disclinations; elastomers; liquid-crystalline polymers (LCP); nematic; microstructure

1 Introduction

Following de Gennes’s prediction¹ of a nematic polymeric material in which orientational and deformational effects are linked, such a material was first successfully synthesized in 1981.² Since then, research into nematic elastomers and other optically active polymers has grown.^{3–9} There has also been a concomitant increase of interest in the role of disclinations^{10–11} and stripes^{12–15}, which can be viewed as defects, in these materials.

This has arisen in large part because of the importance of singularities in traditional nematic liquid crystals, which serve as an exemplar for the study of defects. Since liquid crystals are capable of sustaining point, line, and surface defects, their study has also had far-reaching consequences on the study of defects in disordered systems, frustrated media, and biological molecules. For example, biological polymers such as DNA, PBLG, and xanthan exhibit textures, most of whose defects are similar to those observed

in cholesteric liquid crystals.¹⁶

Contrary to the implication of their name, defects in liquid crystals can be advantageous and, in fact, necessary for the material to exhibit certain phases. They are being harnessed in the zenithal bistable display, which, unlike traditional LCD displays, doesn’t require sustained power to retain an image.^{17–18} Also, the presence of defects is necessary for the stabilization of some of the blue phases observed in cholesteric liquid crystals, wherein the regular three-dimensional lattice is actually composed of disclination lines.^{16,19} In addition, recent research has shown the important effect of disclinations on the reduction of the nematic-isotropic phase transition temperature in nematic liquid-crystals.^{17,20–21}

A disclination in a nematic liquid-crystal is a line along which the orientation is undefined. In the Oseen–Zöcher–Frank (OZF) theory,^{22–24} a non-integrable singularity in the free-energy density occurs at a disclination. Initially, this difficulty was addressed by positing a core of fixed radius and energy about the disclination. However, the fixed energy approach gives no information about the magnitude and energy of the core and also fails to elucidate the underlying physical nature of the core.^{21,25} Nevertheless, for nematics confined to capillaries, it has been shown that the orientation can ‘escape into the third dimension’ at the singularity, thus obviating the need for a core but not ruling one out altogether.^{16,26–28} This deficiency of the OZF theory led Ericksen²⁵ to develop a regularized theory involving the degree-of-orientation, a scalar field which vanishes at disclinations and enters the free energy density in a manner that mollifies the singularity otherwise associated with a disclination. Exploiting this idea, researchers have obtained values of the core radius and energy of a disclination in a cylindrical configuration.^{17,20–21}

Because of the importance of defects in nematic melts, we expect defects to play a similarly influential role in nematic elastomers. In addition, for tech-

nological advances to occur with these materials, a thorough understanding of their defects is necessary.

Previously,^{10–11} we used a continuum model to investigate the existence of disclinations of strength +1 induced by the isochoric distortion of a right circular cylindrical specimen composed of a nematic elastomer that is cross-linked in a uniaxial state and then annealed. Here, we focus on the problem of radial expansion and propose a practical method to determine when a disclinated state exists and, thus, test the predictions of our model.

2 Theory

We confine our attention to uniaxial nematic elastomers. In such materials, the molecular conformation at each material point is that of an ellipsoid of revolution and is completely described by a scalar asphericity $q > -1$ and orientation \mathbf{n} with $|\mathbf{n}| = 1$. For $-1 < q < 0$, the chains are oblate about \mathbf{n} , spherical for $q = 0$, and prolate about \mathbf{n} for $q > 0$. Supplemental to the deformation \mathbf{y} , which describes the distortion of the network, q and \mathbf{n} have the status of additional kinematic degrees of freedom. Consistent with the rubbery nature of nematic elastomers, we require that the deformation be isochoric. This implies that the deformation gradient $\mathbf{F} = \text{Grad} \mathbf{y}$ is subject to the constraint $\det \mathbf{F} = 1$.

We consider a nematic elastomer that is formed by a two-step process and specialize our theory accordingly. Specifically, we suppose that the melt is cross-linked in a uniaxial state with asphericity q_* . Then, we presume that the elastomer is annealed, giving rise to an isotropic reference state in which the conformation at each material point is spherical. We assume that the material retains “memory” of the asphericity at the time of cross-linking, but that the annealing process destroys the orientation associated with this asphericity. To describe such a material, we rely on a free-energy density,

$$\psi = \frac{\mu}{2} \left((1+q)^{\frac{1}{3}} \left(|\mathbf{F}|^2 - \frac{q}{1+q} |\mathbf{F}^\top \mathbf{n}|^2 \right) - 3 \right) + \Phi(q) + \frac{\alpha}{2} |\mathbf{h}|^2 + \Gamma(q) K(\mathbf{F}, \mathbf{n}, \mathbf{G}), \quad (1)$$

which accounts for coupled interactions between the distortion of the network, the asphericity of the molecular conformation, and the orientation of the axis of the molecular conformation. Here, $\mu > 0$ is the *rubber-elasticity modulus*; $\mathbf{G} = \text{Grad} \mathbf{n}$ is the orientation gradient; Φ is a double-well potential, with minima at $q = 0$ and $q = q_*$, consistent with

$$\Phi(q) \rightarrow +\infty \quad \text{as } q \rightarrow -1, +\infty; \quad (2)$$

$\alpha > 0$ is a *regularizing modulus*; $\mathbf{h} = \text{Grad} q$ the asphericity gradient; Γ is a mollifying factor, dimensionless and consistent with

$$\left. \begin{aligned} \Gamma(q) &= O(q^2) \quad \text{as } q \rightarrow 0, \\ \Gamma(q) &> 0 \quad \text{for } q \neq 0, \\ \Gamma(q) &\rightarrow +\infty \quad \text{as } q \rightarrow -1, +\infty; \end{aligned} \right\} \quad (3)$$

and K has the form

$$\begin{aligned} K(\mathbf{F}, \mathbf{n}, \mathbf{G}) &= \frac{\kappa_1}{2} (\mathbf{F} \cdot \mathbf{G})^2 + \frac{\kappa_2}{2} |\mathbf{F}^\top \mathbf{G}|^2 \\ &+ \frac{\kappa_3 (|\mathbf{F}^\top \mathbf{G} \mathbf{F}^\top \mathbf{n}|^2 + |\mathbf{G}^\top \mathbf{F} \mathbf{F}^\top \mathbf{n}|^2)}{2 |\mathbf{F}^\top \mathbf{n}|^2} \\ &+ \frac{\kappa_4}{2} (\mathbf{F}^\top \mathbf{G}) \cdot (\mathbf{G}^\top \mathbf{F}) \\ &+ \frac{\kappa_5 (\mathbf{F}^\top \mathbf{G} \mathbf{F}^\top \mathbf{n}) \cdot (\mathbf{G}^\top \mathbf{F} \mathbf{F}^\top \mathbf{n})}{2 |\mathbf{F}^\top \mathbf{n}|^2}, \quad (4) \end{aligned}$$

involving *orientational-elasticity moduli* $\kappa_1 > 0$, $\kappa_2 > 0$, $\kappa_3 > 0$, $\kappa_4 > 0$, and $\kappa_5 > 0$.

The first term on the right side of (1) is simply the molecular-statistical expression of Warner et al.²⁹ specialized in accordance with the isotropy of the reference state and the uniaxiality of the molecular conformation. The double-well potential accounts for the memory of the asphericity q_* present at the time of cross-linking; together with the regularizing term quadratic in the asphericity gradient, this potential allows for the existence of equilibrium states in which the asphericity is inhomogeneous. The factor K of the final term on the right side of (1) generalizes the energy density of the OZF theory to account for deformation. On setting $\mathbf{F} = \mathbf{1}$ in (4), we may identify $\kappa_1 + \kappa_2 + \kappa_4$, κ_2 , $\kappa_2 + \kappa_3$, and $\kappa_2 + \kappa_4$ with the classical splay, twist, bend, and saddle-splay moduli of the OZF theory; $\kappa_3 + \kappa_5$ is an additional modulus that accounts for interactions between the distortion of the network and the orientation of the molecular conformation. Both Φ and Γ penalize states in which the asphericity limits toward the extreme values $q = -1$ and $q = \infty$. A disclination in a nematic elastomer is an isolated curve along which the asphericity vanishes and the orientation is undefined. The orientation gradient and, hence, K are therefore singular along a disclination. The mollifying factor Γ of the final term on the right side of (1) is introduced to render any such singularities integrable.²⁵

Two sources of coupling between deformation and orientation appear in (1). In the first term on the right side of (1), the nature of the coupling is dictated by molecular-statistical considerations. In the final term on the right side of (1), the nature of the

coupling is dictated by the requirement that K be quadratic in \mathbf{G} , properly invariant and symmetric, and reduce to the OZF energy-density in the absence of deformations.

Granted (1) and that external body forces are absent, the variationally-based equilibrium equations of the theory are

$$\left. \begin{aligned} \text{Div} \left(\frac{\partial \psi}{\partial \mathbf{F}} \right) &= \mathbf{F}^{-\top} \text{Grad} p, \\ \text{Div} \left(\frac{\partial \psi}{\partial \mathbf{h}} \right) &= \frac{\partial \psi}{\partial q}, \\ \text{Div} \left(\frac{\partial \psi}{\partial \mathbf{G}} \right) + \left(\frac{\partial \psi}{\partial \mathbf{G}} \cdot \mathbf{G} \right) \mathbf{n} &= \frac{\partial \psi}{\partial \mathbf{n}}, \end{aligned} \right\} \quad (5)$$

where all differentiation of ψ is performed on the manifold associated with the constraints $\det \mathbf{F} = 1$ and $|\mathbf{n}| = 1$, and where p denotes the pressure. While (5)₁ expresses conventional balance of force associated with \mathbf{y} , (5)₂ and (5)₃ express generalized force balances associated, respectively, with the additional kinematical degrees of freedom q and \mathbf{n} .

Following previous work,¹¹ we use the theory to investigate the presence of disclinations of strength +1 in a nematic-elastomeric specimen which, in the reference state, occupies the right circular cylinder

$$\mathcal{R} = \{\mathbf{x} = r\mathbf{e}_r + z\mathbf{e}_z : 0 \leq r < R, |z| < \infty\}, \quad (6)$$

with cylindrical coordinates (r, θ, z) and $\{\mathbf{e}_r, \mathbf{e}_\theta, \mathbf{e}_z\}$ the associated physical basis. In so doing, we assume that the lateral surface $\partial\mathcal{R} = \{\mathbf{x} : |\mathbf{x}| = R\}$ of the specimen is free of all tractions, viz.,

$$\left. \begin{aligned} \left(\frac{\partial \psi}{\partial \mathbf{F}} - p\mathbf{F}^{-\top} \right) \Big|_{\partial\mathcal{R}} \mathbf{e}_r &= \mathbf{0}, \\ \frac{\partial \psi}{\partial \mathbf{h}} \Big|_{\partial\mathcal{R}} \cdot \mathbf{e}_r &= 0, \quad \frac{\partial \psi}{\partial \mathbf{G}} \Big|_{\partial\mathcal{R}} \mathbf{e}_r &= \mathbf{0}. \end{aligned} \right\} \quad (7)$$

Consistent with the requirement that the deformation be isochoric, we stipulate that it have the form

$$\mathbf{y}(r, \theta, z) = A r \mathbf{e}_r + \frac{z}{A^2} \mathbf{e}_z, \quad \text{with } A > 1, \quad (8)$$

so that the cylinder expands radially while contracting along its axis.* From (8),

$$\mathbf{F}(r, \theta, z) = A(\mathbf{1} - \mathbf{e}_z \otimes \mathbf{e}_z) + \frac{1}{A^2} \mathbf{e}_z \otimes \mathbf{e}_z, \quad (9)$$

and a direct calculation shows that the constraint $\det \mathbf{F} = 1$ holds throughout \mathcal{R} .

We suppose that the orientation is either radial, viz.,

$$\mathbf{n} = \mathbf{e}_r, \quad (10)$$

*The case $0 < A < 1$, for which the cylinder extends along its axis and contracts radially, is discussed elsewhere.¹⁰

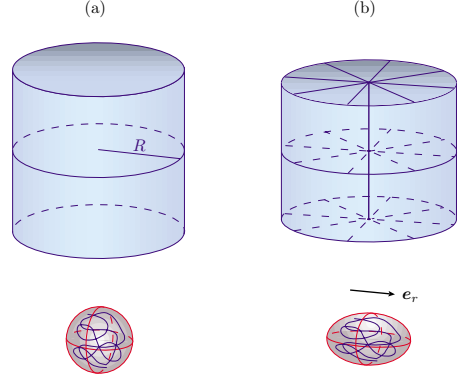


Figure 1: Cylinder and molecular conformation in undistorted (a) and distorted (b) states.

or, as would be the case when $q = 0$, undefined. As a consequence of this choice, the constraint $|\mathbf{n}| = 1$ is satisfied whenever \mathbf{n} is defined. A direct calculation shows that, when \mathbf{n} is defined,

$$\mathbf{G}(r, \theta, z) = \frac{1}{r} \mathbf{e}_\theta \otimes \mathbf{e}_\theta. \quad (11)$$

Further, we suppose that the asphericity q depends at most on the radial coordinate r .

Using (9)–(11) gives

$$K(\mathbf{F}, \mathbf{n}, \mathbf{G}) = \frac{\kappa A^2}{r^2}, \quad (12)$$

with $\kappa = \kappa_1 + \kappa_2 + \kappa_4$ the *orientational-splay modulus*.

Since the deformation is prescribed via (8) and the orientation either has the radial form (10) or is undefined, the only unknowns are the pressure p and asphericity q . From the azimuthal and axial components of (5)₁ and (7)₁ and the assumption that q depends at most on r , it follows that p also may depend at most on r .

Letting ν be a parameter proportional to the height of the barrier separating the minima of the double-well potential Φ and introducing $x = r/R$, $P(x) = p(Rx)/\nu$, and $Q(x) = q(Rx)$, we obtain the dimensionless groups

$$\mu^* = \frac{\mu}{\nu}, \quad \kappa^* = \frac{\kappa}{R^2 \nu}, \quad \text{and} \quad \alpha^* = \frac{\alpha}{R^2 \nu}. \quad (13)$$

Using the radial components of (5)₁ and (7)₁, we find that the dimensionless pressure P has the form

$$P = A^2 (\mu^* ((1 + Q)^{-\frac{2}{3}} + I_1) + \kappa^* I_2), \quad (14)$$

with

$$\left. \begin{aligned} I_1(x) &= \int_x^1 \frac{Q(\xi) d\xi}{\xi(1+Q(\xi))^{\frac{2}{3}}}, \\ I_2(x) &= \int_x^1 \frac{\Gamma(Q(\xi)) d\xi}{\xi^3}. \end{aligned} \right\} \quad (15)$$

From (5)₂, we obtain the differential equation

$$\frac{\alpha^*}{x} \frac{d}{dx} \left(x \frac{dQ}{dx} \right) = \frac{\mu^* A^2}{6(1+Q)^{\frac{2}{3}}} \left(\frac{1}{A^6} - \frac{1-Q}{1+Q} \right) + \frac{\kappa^* A^2 \Gamma'(Q)}{x^2} + \frac{\Phi'(Q)}{\nu}, \quad (16)$$

which is supplemented by boundary conditions,

$$\left. \frac{dQ}{dx} \right|_{x=0} = 0 \quad \text{and} \quad \alpha^* \left. \frac{dQ}{dx} \right|_{x=1} = 0, \quad (17)$$

arising, respectively, from the assumed radial symmetry of the solution and (7)₂.

When $q = 0$ and \mathbf{n} is undefined, (5)₃ and (7)₃ are vacuous. Further, when $q \neq 0$ and $\mathbf{n} = \mathbf{e}_r$, direct calculations show that (5)₃ and (7)₃ are satisfied.

3 Numerical Results

The differential equation (16) involves functions Φ and Γ , which are restricted only by (2) and (3). For our numerical investigations, we took

$$\Phi(q) = \frac{\nu q^2 (q - q_*)^2}{2(1+q)^2}, \quad (18)$$

where, as stated before, $\nu > 0$ determines the height of the energy barrier between states with $q = 0$ and $q = q_*$, and

$$\Gamma(q) = \begin{cases} \frac{q^2}{(1+q)^2} & \text{if } -1 < q \leq 0, \\ q^2 & \text{if } q \geq 0. \end{cases} \quad (19)$$

We emphasize that the particular forms for (18) and (19) are pragmatically based. In particular, because its wells are of equal height, the choice (18) is very special. While defined piecewise, the particular choice (19) of Γ is twice continuously-differentiable. Since (16) involves only the first derivative of Γ , we therefore expect no numerical difficulties to ensue from this choice.

Since the deformation in (8) is restricted to radial expansion ($A > 1$), we expect that the molecular conformation should become prolate in directions perpendicular to the cylinder axis. Thus, it is natural

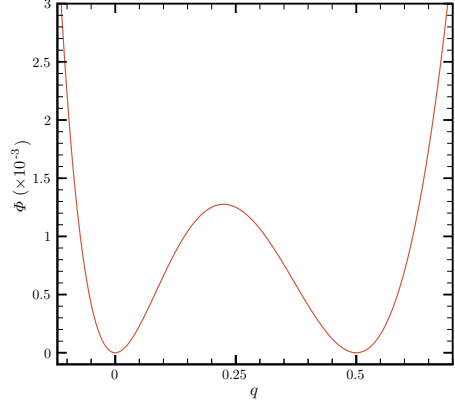


Figure 2: Plot of Φ , as defined in (18) for $\nu = 10^6$ J/m³ and $q_* = 0.5$.

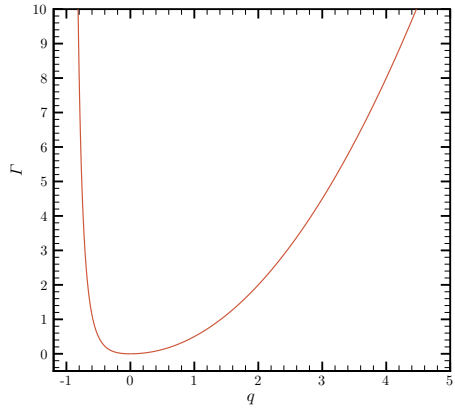


Figure 3: Plot of Γ , as defined in (19).

to restrict $q_* > 0$. Otherwise, there would be no reason for a disclination to form. However, in the case ($0 < A < 1$) where the cylinder is extended along its axis, the molecular conformation would be oblate about the radial direction, and it would be natural to restrict q_* to lie between -1 and 0 .¹⁰

Using (18) and (19), we solved the boundary-value problem (16)–(17) numerically from $x = 0$ to $x = 1$ using the ACDC package³⁰ with the tolerance on the solution of Q set to 10^{-8} and that of its derivative dQ/dx set to 10^{-4} . In so doing, we chose $\mu = 10^5$ J/m³, $\nu = 10^6$ J/m³, $\kappa = \alpha = 10^{-11}$ J/m, and $R = 1$ cm. The values of μ and κ are physically realistic and in line with previous work.⁸ Underlying the chosen value of ν is the notion that, whereas μ should scale like $k_B \theta$ per polymer chain, with k_B Boltzmann's constant and θ the absolute temperature, ν should scale like $k_B \theta$ per monomer. To attain the high extensibilities associated with rubber-like behavior requires upwards of 15–100 monomers per chain, whereby ν should exceed μ by at least an

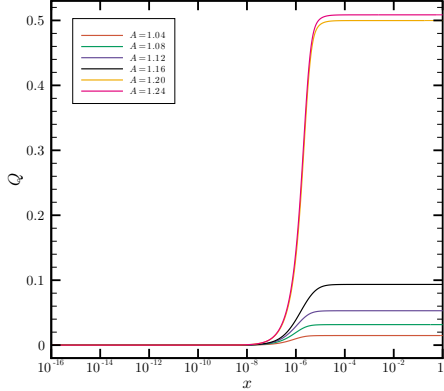


Figure 4: Plots of the asphericity Q as a function of dimensionless radial position x (note logarithmic scale) for the dimensionless material parameters $\mu^* = 0.1$, $\kappa^* = \alpha^* = 10^{-13}$, and $q_* = 0.5$ and representative values of the degree A of radial expansion between 1 and 1.25. Consistent with (17), note the horizontal slopes at the cylinder center ($x = 0$) and outer boundary ($x = 1$). A state connecting the energetically preferred values 0 and q_* of the asphericity is generated for $A \approx 1.20$.

order of magnitude. As a result of these choices, $\mu^* = 10^{-1}$ and $\kappa^* = \alpha^* = 10^{-13}$. Further, for illustrative purposes, we took $q_* = 0.5$. As our initial, trial solution, we used the straight line $Q = 0$, satisfying (17) and consisting of 5001 evenly spaced points on the closed domain. The only parameter varied was A , the degree of radial expansion, which we allowed to range between 1 and 1.25. Figure 4 shows a sharp transition between isotropic ($Q = 0$) and anisotropic ($Q \neq 0$) regions along the cylinder radius, thereby indicating the presence of a disclination of strength $+1$ located along the cylinder axis. The extent of the disclination core can also be inferred from the plot as the region where Q exhibits a rapid increase.²¹ From Figure 4, the center of the transition zone appears to be at $x = 10^{-6}$, which corresponds to a dimensional core radius on the order of $10^{-2} \mu\text{m}$ and is consistent with the length scale predicted by the ratio $\sqrt{\kappa/\mu}$ for our choices of μ and κ .[†] A closer examination of the solution curves places the center of the layer at $x = 1.5 \times 10^{-6}$ (corresponding to a core radius of $0.015 \mu\text{m}$), which we associate with the core boundary and denote by x_c . Our core radius is of the same order as values observed for liquid crystalline melts.³¹

[†]The ratio $\sqrt{\kappa/\mu}$ determines the length scale at which a cross-over between rubber-elastic and orientational effects occurs. As discussed in the literature,^{12–13,15} this ratio plays an important role in the formation of striped microstructures in nematic elastomers.

To discuss energetic issues, we introduce the dimensionless free-energy density $\Psi = \psi/\nu$. In view of our assumptions concerning \mathbf{F} , \mathbf{n} , and q ,

$$\Psi = \frac{\psi}{\nu} = \Psi_e + \Psi_a + \Psi_o, \quad (20)$$

with

$$\Psi_e = \frac{\mu^*}{2} \left(2A^2 + \frac{1}{A^4} - 3 \right), \quad (21)$$

a conventional neo-Hookean rubber-elastic contribution associated with the distortion of the network,

$$\Psi_a = \frac{\mu^*}{2} \left(A^2 \left(\frac{2+Q}{(1+Q)^{\frac{2}{3}}} - 2 \right) + \frac{1}{A^4} \left((1+Q)^{\frac{1}{3}} - 1 \right) \right) + \frac{\Phi(Q)}{\nu} + \frac{\alpha^*}{2} \left(\frac{dQ}{dx} \right)^2 \quad (22)$$

a contribution associated with the asphericity of the molecular conformation, and

$$\Psi_o = \frac{\kappa^* A^2 \Gamma(Q)}{2x^2} \quad (23)$$

a contribution associated with the axis of the molecular conformation.

A comparison of the total neo-Hookean energy

$$\mathcal{F}_e^{\text{tot}} = \int_0^1 \Psi_e(x) x dx \quad (24)$$

and total energy

$$\mathcal{F}^{\text{tot}} = \int_0^1 \Psi(x) x dx \quad (25)$$

plotted in Figure 5 shows why a disclination forms. While $\mathcal{F}_e^{\text{tot}}$ increases monotonically with A , \mathcal{F}^{tot} is a double-well potential with an absolute minimum at $A = 1$ and a relative minimum at $A \approx 1.17$. Also, for all $A > 1$, \mathcal{F}^{tot} is less than $\mathcal{F}_e^{\text{tot}}$, the isotropic ($Q = 0$) neo-Hookean contribution alone. This difference is negligible for all $A \leq 1.16$, and we therefore do not necessarily expect a disclination to form in this range. However, beyond $A = 1.16$, the difference between \mathcal{F}^{tot} and $\mathcal{F}_e^{\text{tot}}$ becomes non-trivial and shows an energetic motivation for the material to form a disclinated region with the remainder of the material beyond x_c in an anisotropic state.

In addition, we investigated the energy of the core, which we denote as

$$\mathcal{F}^{\text{core}} = \int_0^{x_c} \Psi(x) x dx, \quad (26)$$

relative to that of the whole domain. From Figure 6, it is evident that $\mathcal{F}^{\text{core}}$ is a vanishingly small percentage of \mathcal{F}^{tot} . This is because of the relatively small size

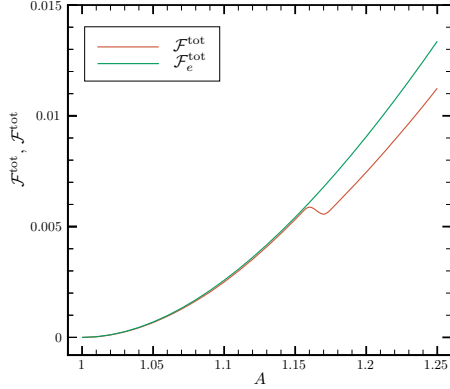


Figure 5: Plots of the total neo-Hookean rubber-elastic energy $\mathcal{F}_e^{\text{tot}}$ and of the total free-energy \mathcal{F}^{tot} as a function of the degree A of radial expansion between 1 and 1.25 for the dimensionless material parameters $\mu^* = 0.1$, $\kappa^* = \alpha^* = 10^{-13}$, and $q_* = 0.5$.

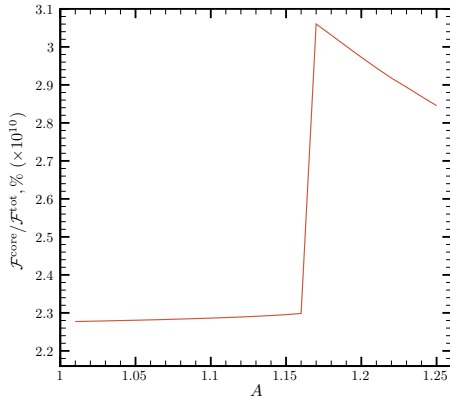


Figure 6: Plot of the percentage $\mathcal{F}^{\text{core}}/\mathcal{F}^{\text{tot}}$ of free energy in the core as a function of the degree A of cylinder distortion between 1 and 1.25 for the dimensionless material parameters $\mu^* = 0.1$, $\kappa^* = \alpha^* = 10^{-13}$, and $q_* = 0.5$.

of the core and the fact that Ψ_e is of a comparatively large magnitude across the entire radial extent of the cylinder. The proportion of total energy contained in the core remains relatively constant up to the value of A corresponding to the first inflection point of the total energy. A sharp increase then occurs, and the proportion then decreases monotonically for the remainder of our range as more energy goes into both stretching of the polymer network and changing the asphericity of the chains comprising the network.

The dimensionless pressure P given in (14) is shown in Figure 7. For each A , P increases monotonically from its minimum at the cylinder's boundary ($x = 1$) until it reaches a maximum at the core

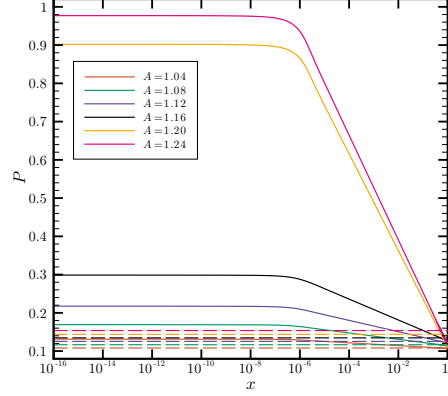


Figure 7: Plot of the dimensionless pressure P as a function of dimensionless radial position x (note logarithmic scale) for the dimensionless material parameters $\mu^* = 0.1$, $\kappa^* = \alpha^* = 10^{-13}$, and $q_* = 0.5$ and representative values of the degree A of radial expansion between 1 and 1.25. Dashed lines show corresponding neo-Hookean values of P .

boundary ($x = x_c$), whereafter it remains essentially constant up to the cylinder axis ($x = 0$). The pressure at the edge is almost the same regardless of the value of A . This occurs because the last two terms of (14) vanish at $x = 1$, so that the pressure there is only dependent on the first term, which doesn't vary significantly for our range of A . For each A , the neo-Hookean ($Q = 0$) pressure is seen to be much less than P for almost the entire domain. However, close to the outer edge of the cylinder, P is actually less than its neo-Hookean counterpart. This is because although the last two terms of (14) are positive, they are negligible in this region and are overwhelmed by the first term which, due to the factor of $(1 + Q)^{\frac{2}{3}}$ in its denominator, decreases below the corresponding neo-Hookean value. Away from the edge though, the last two terms of (14) overwhelm the first, and so the pressure exceeds the neo-Hookean value.

To discuss normal-stress differences, we introduce the dimensionless Cauchy stress[‡]

$$\mathbf{T} = \frac{1}{\nu} \frac{\partial \psi}{\partial \mathbf{F}} \mathbf{F}^T - P \mathbf{1}. \quad (27)$$

Our assumptions concerning \mathbf{F} , \mathbf{n} , and q yield $\mathbf{T} =$

[‡]In writing (27), we take advantage of the constraint $\det \mathbf{F} = 1$.

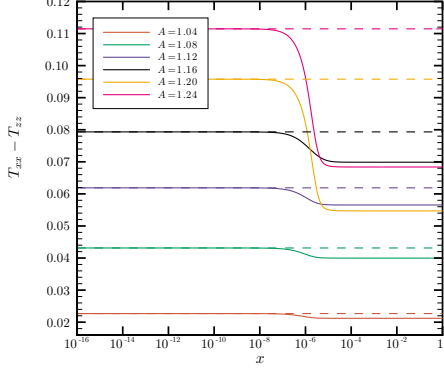


Figure 8: Plots of the first normal-stress difference $T_{xx} - T_{zz}$ (solid lines) and its neo-Hookean counterpart (dashed lines) as a function of dimensionless radial position x (note logarithmic scale) for the dimensionless material parameters $\mu^* = 0.1$, $\kappa^* = \alpha^* = 10^{-13}$, and $q_* = 0.5$.

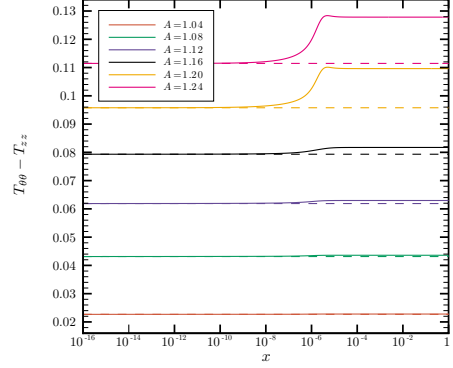


Figure 9: Plots of the second normal-stress difference $T_{\theta\theta} - T_{zz}$ (solid lines) and its neo-Hookean counterpart (dashed lines) as a function of dimensionless radial position x (note logarithmic scale) for the dimensionless material parameters $\mu^* = 0.1$, $\kappa^* = \alpha^* = 10^{-13}$, and $q_* = 0.5$.

$T_{xx}\mathbf{e}_r \otimes \mathbf{e}_r + T_{\theta\theta}\mathbf{e}_\theta \otimes \mathbf{e}_\theta + T_{zz}\mathbf{e}_z \otimes \mathbf{e}_z$, with

$$\left. \begin{aligned} T_{xx} &= \frac{\mu^* A^2}{(1+Q)^{\frac{2}{3}}} - P, \\ T_{\theta\theta} &= \mu^* A^2 (1+Q)^{\frac{1}{3}} + \frac{\kappa^* A \Gamma(Q)}{x^2} - P, \\ T_{zz} &= \frac{\mu^* (1+Q)^{\frac{1}{3}}}{A^4} - P. \end{aligned} \right\} \quad (28)$$

The first and second normal-stress differences $T_{xx} - T_{zz}$ and $T_{\theta\theta} - T_{zz}$ are computed from (28) and (19)₂ and plotted in Figures 8 and 9. In addition, for each A , the value of $T_{xx} - T_{zz}$ at the cylinder edge ($x = 1$) is plotted in Figure 10. Within the core, these differences coincide with their neo-Hookean counterparts. Outside the core, however, $T_{xx} - T_{zz}$ and $T_{\theta\theta} - T_{zz}$ take values that lie below their neo-Hookean counterparts. Most strikingly, from Figure 10, we see that there is a local minimum in the first normal-stress difference at $A = 1.16$. This local minimum coincides both with the decrease of \mathcal{F}^{tot} in Figure 5 and increase of $\mathcal{F}^{\text{core}}/\mathcal{F}^{\text{tot}}$ in Figure 6 at $A = 1.16$ and provides further evidence that a disclinated state has been achieved. Based on this non-monotonicity, an experiment designed to measure normal stress differences under a radial expansion of the sort considered here could be used as a practical means to detect the presence of a disclination and, thereby, the predictions of our model.

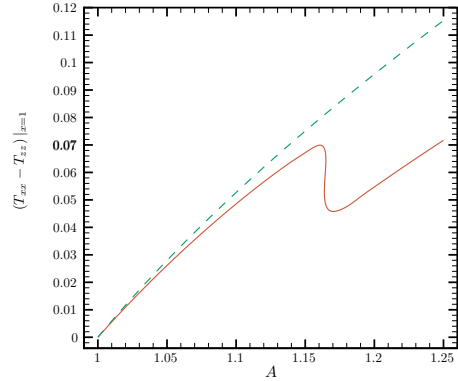


Figure 10: Plots of the value of the first normal-stress difference $T_{xx} - T_{zz}$ (solid line) and its neo-Hookean counterpart (dashed line) at the boundary of the specimen ($x = 1$) as a function of the degree A of radial expansion between 1 and 1.25 for the dimensionless material parameters $\mu^* = 0.1$, $\kappa^* = \alpha^* = 10^{-13}$, and $q_* = 0.5$.

4 Discussion

In addition to predicting that nematic elastomers are capable of sustaining disclinations, our model yields information concerning the characteristic dimension of the core of a disclination of strength $+1$ and determines the distributions of energy and stress in disclinated states. Energetic considerations show that, above a certain deformational threshold, the material prefers disclinated states. Based on the behavior of the first normal-stress difference, the model additionally suggests a practical experimental method by which its predictions can be tested.

Our restriction to nematic elastomers with uniaxial molecular conformation rules out the possibility of biaxial states. Hence, for the problem of a cylinder distorted in the manner considered here, it is possible that there may exist disclinated states in which the conformation becomes biaxial in the region outside the core and that for certain values of radial expansion, such states may be energetically favored over the uniaxial states discussed here.

While our predictions are confined to nematic elastomers which have been specially prepared, we speculate that disclinations may occur under other circumstances and that normal-stress measurements may provide a convenient vehicle for determining when that is the case.

Acknowledgments

We thank Don Carlson and Mark Warner for many valuable discussions. This work was supported by the National Science Foundation and the Department of Energy.

References

1. de Gennes, P.G. *C R Seances Acad Sci B* 1975, 281, 101–103.
2. Finkelmann, H.; Kock, H.-J.; Rehage, G. *Makromol Chem Rapid Commun* 1981, 2, 317–322.
3. Anderson, D.R.; Carlson, D.E.; Fried, E. *J Elasticity* 1999, 56, 33–58.
4. DeSimone A.; Dolzmann, G. *Physica D* 2000, 136, 175–191.
5. Davis, F.J. *J Mater Chem* 1993, 3, 551–562.
6. Finkelmann, H. *Angew Chem Adv Mater* 1988, 100, 1019–1020.
7. Terentjev, E.M. *J Phys Condens Matter* 1999, 11, R239–R257.
8. Warner, M.; Terentjev, E.M. *Prog Polym Sci* 1996, 21, 853–891.
9. Zentel, R. *Angew Chem Adv Mater* 1989, 101, 1437–1445.
10. Fried, E.; Todres, R.E. *Proc Natl Acad Sci USA* 2001, 98, 14773–14777.
11. Fried, E.; Todres, R.E. *J Mech Phys Solids* 2002, in press.
12. Verwey, G.C.; Warner, M.; Terentjev, E.M. *J Phys II* 1996, 6, 1273–1290.
13. Finkelmann, H.; Kundler, I.; Terentjev, E.M.; Warner, M. *J Phys II* 1997, 7, 1059–1069.
14. Conti, S.; DeSimone, A.; Dolzmann, G. *J Mech Phys Solids* 2002, in press.
15. Fried, E.; Korchagin, V. *Int J Solids Struct* 2002, in press.
16. Kléman, M. *Rep Prog Phys* 1989, 52, 555–654.
17. Mottram, N.J.; Sluckin, T.J. *Liq Cryst* 2000, 27, 1301–1304.
18. Jones, J.C.; Graham, A.; Bryan-Brown, G.P.; Wood, E.P.; Brett, P. 2000 Proceedings of ASET International Forum on Low Power Displays, Tokyo, 17–24.
19. Chandrasekhar, S. *Contemp Phys* 1988, 29, 527–558.
20. Adrienko, D.; Allen, M.P. *Phys Rev E* 61, 504–510.
21. Mottram, N.J.; Hogan, S.J. *Philos Trans R Soc London, Ser A* 1997, 355, 2045–2064.
22. Oseen, W.C. *Trans Faraday Soc* 1933, 29, 883–899.
23. Zöcher, H. *Trans Faraday Soc* 1933, 29, 945–957.
24. Frank, F.C. *Discuss Faraday Soc* 1958, 250, 19–28.
25. Ericksen, J.L. *Arch Rational Mech Anal* 1991, 113, 97–120.
26. Cladis, P.E.; Kléman, M. *J Phys* 1972, 33, 591–598.
27. Meyer, R.B. *Phil Mag* 1973, 27, 405–424.
28. Williams, C.; Pierański, P.; Cladis, P.E. *Phys Rev Lett* 1972, 29, 90–92.
29. Warner, M.; Gelling, K.P.; Vilgis, T.A. *J Chem Phys* 1988, 88, 4008–4013.
30. Cash, J.R.; Wright, R.W. *Appl Numer Math* 1988, 28, 227–244.
31. Chandrasekhar, S.; Ranganath, G.S. *Adv Phys* 1986, 35, 507–596.

List of Recent TAM Reports

No.	Authors	Title	Date
920	Block, G. I., J. G. Harris, and T. Hayat	Measurement models for ultrasonic nondestructive evaluation – <i>IEEE Transactions on Ultrasonics, Ferroelectrics, and Frequency Control</i> 47 , 604–611 (2000)	Sept. 1999
921	Zhang, S., and K. J. Hsia	Modeling the fracture of a sandwich structure due to cavitation in a ductile adhesive layer – <i>Journal of Applied Mechanics</i> 68 , 93–100 (2001)	Sept. 1999
922	Nimmagadda, P. B. R., and P. Sofronis	Leading order asymptotics at sharp fiber corners in creeping-matrix composite materials	Oct. 1999
923	Yoo, S., and D. N. Riahi	Effects of a moving wavy boundary on channel flow instabilities – <i>Theoretical and Computational Fluid Dynamics</i> (submitted)	Nov. 1999
924	Adrian, R. J., C. D. Meinhart, and C. D. Tomkins	Vortex organization in the outer region of the turbulent boundary layer – <i>Journal of Fluid Mechanics</i> 422 , 1–53 (2000)	Nov. 1999
925	Riahi, D. N., and A. T. Hsui	Finite amplitude thermal convection with variable gravity – <i>International Journal of Mathematics and Mathematical Sciences</i> 25 , 153–165 (2001)	Dec. 1999
926	Kwok, W. Y., R. D. Moser, and J. Jiménez	A critical evaluation of the resolution properties of B-spline and compact finite difference methods – <i>Journal of Computational Physics</i> (submitted)	Feb. 2000
927	Ferry, J. P., and S. Balachandar	A fast Eulerian method for two-phase flow – <i>International Journal of Multiphase Flow</i> , in press (2000)	Feb. 2000
928	Thoroddsen, S. T., and K. Takehara	The coalescence-cascade of a drop – <i>Physics of Fluids</i> 12 , 1257–1265 (2000)	Feb. 2000
929	Liu, Z.-C., R. J. Adrian, and T. J. Hanratty	Large-scale modes of turbulent channel flow: Transport and structure – <i>Journal of Fluid Mechanics</i> 448 , 53–80 (2001)	Feb. 2000
930	Borodai, S. G., and R. D. Moser	The numerical decomposition of turbulent fluctuations in a compressible boundary layer – <i>Theoretical and Computational Fluid Dynamics</i> (submitted)	Mar. 2000
931	Balachandar, S., and F. M. Najjar	Optimal two-dimensional models for wake flows – <i>Physics of Fluids</i> , in press (2000)	Mar. 2000
932	Yoon, H. S., K. V. Sharp, D. F. Hill, R. J. Adrian, S. Balachandar, M. Y. Ha, and K. Kar	Integrated experimental and computational approach to simulation of flow in a stirred tank – <i>Chemical Engineering Sciences</i> 56 , 6635–6649 (2001)	Mar. 2000
933	Sakakibara, J., Hishida, K., and W. R. C. Phillips	On the vortical structure in a plane impinging jet – <i>Journal of Fluid Mechanics</i> 434 , 273–300 (2001)	Apr. 2000
934	Phillips, W. R. C.	Eulerian space-time correlations in turbulent shear flows – <i>Physics of Fluids</i> 12 , 2056–2064 (2000)	Apr. 2000
935	Hsui, A. T., and D. N. Riahi	Onset of thermal-chemical convection with crystallization within a binary fluid and its geological implications – <i>Geochemistry, Geophysics, Geosystems</i> 2 , 2000GC000075 (2001)	Apr. 2000
936	Cermelli, P., E. Fried, and S. Sellers	Configurational stress, yield, and flow in rate-independent plasticity – <i>Proceedings of the Royal Society of London A</i> 457 , 1447–1467 (2001)	Apr. 2000
937	Adrian, R. J., C. Meneveau, R. D. Moser, and J. J. Riley	Final report on ‘Turbulence Measurements for Large-Eddy Simulation’ workshop	Apr. 2000
938	Bagchi, P., and S. Balachandar	Linearly varying ambient flow past a sphere at finite Reynolds number – Part 1: Wake structure and forces in steady straining flow	Apr. 2000
939	Gioia, G., A. DeSimone, M. Ortiz, and A. M. Cuitiño	Folding energetics in thin-film diaphragms – <i>Proceedings of the Royal Society of London A</i> 458 , 1223–1229 (2002)	Apr. 2000

List of Recent TAM Reports (cont'd)

No.	Authors	Title	Date
940	Chaïeb, S., and G. H. McKinley	Mixing immiscible fluids: Drainage induced cusp formation	May 2000
941	Thoroddsen, S. T., and A. Q. Shen	Granular jets – <i>Physics of Fluids</i> 13 , 4–6 (2001)	May 2000
942	Riahi, D. N.	Non-axisymmetric chimney convection in a mushy layer under a high-gravity environment – In <i>Centrifugal Materials Processing</i> (L. L. Regel and W. R. Wilcox, eds.), 295–302 (2001)	May 2000
943	Christensen, K. T., S. M. Soloff, and R. J. Adrian	PIV Sleuth: Integrated particle image velocimetry interrogation/validation software	May 2000
944	Wang, J., N. R. Sottos, and R. L. Weaver	Laser induced thin film spallation – <i>Experimental Mechanics</i> (submitted)	May 2000
945	Riahi, D. N.	Magneto-hydrodynamic effects in high gravity convection during alloy solidification – In <i>Centrifugal Materials Processing</i> (L. L. Regel and W. R. Wilcox, eds.), 317–324 (2001)	June 2000
946	Gioia, G., Y. Wang, and A. M. Cuitiño	The energetics of heterogeneous deformation in open-cell solid foams – <i>Proceedings of the Royal Society of London A</i> 457 , 1079–1096 (2001)	June 2000
947	Kessler, M. R., and S. R. White	Self-activated healing of delamination damage in woven composites – <i>Composites A: Applied Science and Manufacturing</i> 32 , 683–699 (2001)	June 2000
948	Phillips, W. R. C.	On the pseudomomentum and generalized Stokes drift in a spectrum of rotational waves – <i>Journal of Fluid Mechanics</i> 430 , 209–229 (2001)	July 2000
949	Hsui, A. T., and D. N. Riahi	Does the Earth's nonuniform gravitational field affect its mantle convection? – <i>Physics of the Earth and Planetary Interiors</i> (submitted)	July 2000
950	Phillips, J. W.	Abstract Book, 20th International Congress of Theoretical and Applied Mechanics (27 August – 2 September, 2000, Chicago)	July 2000
951	Vainchtein, D. L., and H. Aref	Morphological transition in compressible foam – <i>Physics of Fluids</i> 13 , 2152–2160 (2001)	July 2000
952	Chaïeb, S., E. Sato-Matsuo, and T. Tanaka	Shrinking-induced instabilities in gels	July 2000
953	Riahi, D. N., and A. T. Hsui	A theoretical investigation of high Rayleigh number convection in a nonuniform gravitational field – <i>Acta Mechanica</i> (submitted)	Aug. 2000
954	Riahi, D. N.	Effects of centrifugal and Coriolis forces on a hydromagnetic chimney convection in a mushy layer – <i>Journal of Crystal Growth</i> 226 , 393–405 (2001)	Aug. 2000
955	Fried, E.	An elementary molecular-statistical basis for the Mooney and Rivlin-Saunders theories of rubber-elasticity – <i>Journal of the Mechanics and Physics of Solids</i> 50 , 571–582 (2002)	Sept. 2000
956	Phillips, W. R. C.	On an instability to Langmuir circulations and the role of Prandtl and Richardson numbers – <i>Journal of Fluid Mechanics</i> 442 , 335–358 (2001)	Sept. 2000
957	Chaïeb, S., and J. Sutin	Growth of myelin figures made of water soluble surfactant – Proceedings of the 1st Annual International IEEE-EMBS Conference on Microtechnologies in Medicine and Biology (October 2000, Lyon, France), 345–348	Oct. 2000
958	Christensen, K. T., and R. J. Adrian	Statistical evidence of hairpin vortex packets in wall turbulence – <i>Journal of Fluid Mechanics</i> 431 , 433–443 (2001)	Oct. 2000
959	Kuznetsov, I. R., and D. S. Stewart	Modeling the thermal expansion boundary layer during the combustion of energetic materials – <i>Combustion and Flame</i> , in press (2001)	Oct. 2000
960	Zhang, S., K. J. Hsia, and A. J. Pearlstein	Potential flow model of cavitation-induced interfacial fracture in a confined ductile layer – <i>Journal of the Mechanics and Physics of Solids</i> , in press (2002)	Nov. 2000

List of Recent TAM Reports (cont'd)

No.	Authors	Title	Date
961	Sharp, K. V., R. J. Adrian, J. G. Santiago, and J. I. Molho	Liquid flows in microchannels – Chapter 6 of <i>CRC Handbook of MEMS</i> (M. Gad-el-Hak, ed.) (2001)	Nov. 2000
962	Harris, J. G.	Rayleigh wave propagation in curved waveguides – <i>Wave Motion</i> , in press (2001)	Jan. 2001
963	Dong, F., A. T. Hsui, and D. N. Riahi	A stability analysis and some numerical computations for thermal convection with a variable buoyancy factor – <i>Journal of Theoretical and Applied Mechanics</i> , in press (2002)	Jan. 2001
964	Phillips, W. R. C.	Langmuir circulations beneath growing or decaying surface waves – <i>Journal of Fluid Mechanics</i> (submitted)	Jan. 2001
965	Bdzil, J. B., D. S. Stewart, and T. L. Jackson	Program burn algorithms based on detonation shock dynamics – <i>Journal of Computational Physics</i> (submitted)	Jan. 2001
966	Bagchi, P., and S. Balachandar	Linearly varying ambient flow past a sphere at finite Reynolds number: Part 2 – Equation of motion – <i>Journal of Fluid Mechanics</i> (submitted)	Feb. 2001
967	Cermelli, P., and E. Fried	The evolution equation for a disclination in a nematic fluid – <i>Proceedings of the Royal Society A</i> 458 , 1–20 (2002)	Apr. 2001
968	Riahi, D. N.	Effects of rotation on convection in a porous layer during alloy solidification – Chapter in <i>Transport Phenomena in Porous Media</i> (D. B. Ingham and I. Pop, eds.), Oxford: Elsevier Science (2001)	Apr. 2001
969	Damljanovic, V., and R. L. Weaver	Elastic waves in cylindrical waveguides of arbitrary cross section – <i>Journal of Sound and Vibration</i> (submitted)	May 2001
970	Gioia, G., and A. M. Cuitiño	Two-phase densification of cohesive granular aggregates – <i>Physical Review Letters</i> 88 , 204302 (2002) (in extended form and with added co-authors S. Zheng and T. Uribe)	May 2001
971	Subramanian, S. J., and P. Sofronis	Calculation of a constitutive potential for isostatic powder compaction – <i>International Journal of Mechanical Sciences</i> (submitted)	June 2001
972	Sofronis, P., and I. M. Robertson	Atomistic scale experimental observations and micromechanical/continuum models for the effect of hydrogen on the mechanical behavior of metals – <i>Philosophical Magazine</i> (submitted)	June 2001
973	Pushkin, D. O., and H. Aref	Self-similarity theory of stationary coagulation – <i>Physics of Fluids</i> 14 , 694–703 (2002)	July 2001
974	Lian, L., and N. R. Sottos	Stress effects in ferroelectric thin films – <i>Journal of the Mechanics and Physics of Solids</i> (submitted)	Aug. 2001
975	Fried, E., and R. E. Todres	Prediction of disclinations in nematic elastomers – <i>Proceedings of the National Academy of Sciences</i> 98 , 14773–14777 (2001)	Aug. 2001
976	Fried, E., and V. A. Korchagin	Striping of nematic elastomers – <i>International Journal of Solids and Structures</i> , in press (2002)	Aug. 2001
977	Riahi, D. N.	On nonlinear convection in mushy layers: Part I. Oscillatory modes of convection – <i>Journal of Fluid Mechanics</i> , in press (2002)	Sept. 2001
978	Sofronis, P., I. M. Robertson, Y. Liang, D. F. Teter, and N. Aravas	Recent advances in the study of hydrogen embrittlement at the University of Illinois – Invited paper, Hydrogen–Corrosion Deformation Interactions (Sept. 16–21, 2001, Jackson Lake Lodge, Wyo.)	Sept. 2001
979	Fried, E., M. E. Gurtin, and K. Hutter	A void-based description of compaction and segregation in flowing granular materials – <i>Proceedings of the Royal Society of London A</i> (submitted)	Sept. 2001
980	Adrian, R. J., S. Balachandar, and Z.-C. Liu	Spanwise growth of vortex structure in wall turbulence – <i>Korean Society of Mechanical Engineers International Journal</i> 15 , 1741–1749 (2001)	Sept. 2001
981	Adrian, R. J.	Information and the study of turbulence and complex flow – <i>Japanese Society of Mechanical Engineers Journal B</i> , in press (2002)	Oct. 2001
982	Adrian, R. J., and Z.-C. Liu	Observation of vortex packets in direct numerical simulation of fully turbulent channel flow – <i>Journal of Visualization</i> , in press (2002)	Oct. 2001

List of Recent TAM Reports (cont'd)

No.	Authors	Title	Date
983	Fried, E., and R. E. Todres	Disclinated states in nematic elastomers – <i>Journal of the Mechanics and Physics of Solids</i> , in press (2002)	Oct. 2001
984	Stewart, D. S.	Towards the miniaturization of explosive technology – Proceedings of the 23rd International Conference on Shock Waves (2001)	Oct. 2001
985	Kasimov, A. R., and Stewart, D. S.	Spinning instability of gaseous detonations – <i>Journal of Fluid Mechanics</i> (submitted)	Oct. 2001
986	Brown, E. N., N. R. Sottos, and S. R. White	Fracture testing of a self-healing polymer composite – <i>Experimental Mechanics</i> (submitted)	Nov. 2001
987	Phillips, W. R. C.	Langmuir circulations – <i>Surface Waves</i> (J. C. R. Hunt and S. Sajjadi, eds.), in press (2002)	Nov. 2001
988	Gioia, G., and F. A. Bombardelli	Scaling and similarity in rough channel flows – <i>Physical Review Letters</i> 88 , 014501 (2002)	Nov. 2001
989	Riahi, D. N.	On stationary and oscillatory modes of flow instabilities in a rotating porous layer during alloy solidification – <i>Journal of Porous Media</i> , in press (2002)	Nov. 2001
990	Okhuysen, B. S., and D. N. Riahi	Effect of Coriolis force on instabilities of liquid and mushy regions during alloy solidification – <i>Physics of Fluids</i> (submitted)	Dec. 2001
991	Christensen, K. T., and R. J. Adrian	Measurement of instantaneous Eulerian acceleration fields by particle-image accelerometry: Method and accuracy – <i>Experimental Fluids</i> (submitted)	Dec. 2001
992	Liu, M., and K. J. Hsia	Interfacial cracks between piezoelectric and elastic materials under in-plane electric loading – <i>Journal of the Mechanics and Physics of Solids</i> (submitted)	Dec. 2001
993	Panat, R. P., S. Zhang, and K. J. Hsia	Bond coat surface rumpling in thermal barrier coatings – <i>Acta Materialia</i> (submitted)	Jan. 2002
994	Aref, H.	A transformation of the point vortex equations – <i>Physics of Fluids</i> (submitted)	Jan. 2002
995	Saif, M. T. A, S. Zhang, A. Haque, and K. J. Hsia	Effect of native Al ₂ O ₃ on the elastic response of nanoscale aluminum films – <i>Acta Materialia</i> (submitted)	Jan. 2002
996	Fried, E., and M. E. Gurtin	A nonequilibrium theory of epitaxial growth that accounts for surface stress and surface diffusion – <i>Journal of the Mechanics and Physics of Solids</i> , in press (2002)	Jan. 2002
997	Aref, H.	The development of chaotic advection – <i>Physics of Fluids</i> 14 , 1315–1325 (2002); see also <i>Virtual Journal of Nanoscale Science and Technology</i> , 11 March 2002	Jan. 2002
998	Christensen, K. T., and R. J. Adrian	The velocity and acceleration signatures of small-scale vortices in turbulent channel flow – <i>Journal of Turbulence</i> , in press (2002)	Jan. 2002
999	Riahi, D. N.	Flow instabilities in a horizontal dendrite layer rotating about an inclined axis – <i>Proceedings of the Royal Society of London A</i> (submitted)	Feb. 2002
1000	Kessler, M. R., and S. R. White	Cure kinetics of ring-opening metathesis polymerization of dicyclopentadiene – <i>Journal of Polymer Science A</i> (submitted)	Feb. 2002
1001	Dolbow, J. E., E. Fried, and Amy Q. Shen	Point defects in nematic gels: The case for hedgehogs – <i>Proceedings of the National Academy of Sciences</i> (submitted)	Feb. 2002
1002	Riahi, D. N.	Nonlinear steady convection in rotating mushy layers – <i>Journal of Fluid Mechanics</i> (submitted)	Mar. 2002
1003	Carlson, D. E., E. Fried, and S. Sellers	The totality of soft-states in a neo-classical nematic elastomer – <i>Proceedings of the Royal Society A</i> (submitted)	Mar. 2002
1004	Fried, E., and Russell E. Todres	Normal-stress differences and the detection of disclinations in nematic elastomers – <i>Journal of Polymer Science B: Polymer Physics</i> , in press (2002)	June 2002